Combined theoretical and experimental approaches for development of squaraine dyes with small energy barrier for electron injection

Combined theoretical and experimental approached for development of squaraiune dyes with small energy barrier for electron injection

Shyam S. Pandey*, Takuya Morimoto, Naotaka Fujikawa and Shuzi Hayase

Graduate School of Life Science and Systems Engineering, Kyushu Institute of Technology, 2-4, Hibikino, Wakamatsu, Kitakyushu, 808-0196, JAPAN

E-mail address: shyam@life.kyutech.ac.jp

ABSTRACT

A series of far-red sensitizing squaraine dyes has been systematically designed and synthesized in order to correlate the theoretically calculated values with their corresponding experimental parameters. Effort have been directed towards determining the minimum thermodynamic energy barrier for the electron injection in the nanoporous TiO_2 by logical molecular design. Theoretical calculations using Gaussian program package were performed in both ground and excited states in both isolated gaseous state as well as including the solvent effect using self-consistent reaction field polarizable continuum model (PCM). Implementation of PCM model or use of LSDA functional under TD-DFT calculations gives much better results for energetics as well as absorption maximum for all the sensitizers used in this work. Newly designed symmetrical squaraine dye SQ-5 exhibits a minimum energy barrier of 0.16 eV for electron injection and shows photon harvesting behavior in far-red region with external photoconversion efficiency of 2.02 % under simulated solar irradiation.

Keywords: Squaraine dyes, Far-red sensitization, Dye-sensitized solar cells, TD-DFT calculation, Energy barrier

1. Introduction

Dye-sensitized solar cells (DSSCs) have seen tremendous growth and received a good deal of attentions from material science community pertaining to the economical and environment friendly solar energy harvesting as compared to traditional silicon based solar cells [1]. Optimization of DSSC performance in terms wide band gap mesoporous semiconductor, potential photosensitizers, redox electrolyte and counter electrodes have led to the attainment of photoconversion efficiency over 10 % similar to amorphous silicon solar cells [2-5]. Last 10 years of research and development have witnessed the appreciable success in the attainment of nearly quantitative photon harvesting by DSSCs utilizing ruthenium complex based inorganic as well as metal free organic sensitizers [6-7]. A perusal of the photoconversion by potential sensitizers used in DSSCs corroborates that it is possible to achieve the photoconversion efficiency beyond 12 % even having photon harvesting mainly in the visible region (400-750 nm) of the solar spectrum [8-9]. This indicates a good hope, potentiality and urgent need for the development of efficient sensitizers having the capability of photon harvesting in NIR-IR wavelength region for the further enhancement in the overall photoconversion efficiency. In this context, efforts are being directed to design and develop far-red to near infra-red (NIR) sensitizers for DSSC application and efficient photosensitization in the far-red region has already been achieved but efficient photosensitization in the NIR region has still to be achieved [10-13].

In spite of having high molar extinction coefficient and suitable anchoring group, a suitable sensitizer for DSSC application must possesses the energetic matching with respect to wide band gap semiconductor and redox electrolyte for facile electron injection and dye regeneration. Since sensitizing dyes a play a pivotal role in controlling the photoconversion efficiency, development of suitable dyes working efficiently in the far-red to near infra-red (NIR) region is still challenging owing to their relatively smaller band gap (Eg) and needs the attentions

of the material science community. Relatively small Eg of NIR sensitizers needs the attention for strict control on the energetics for their optimal functioning and a judicious molecular design is necessary. Taking model far-red sensitive squaraine dyes we have recently demonstrated that it is possible to control of energetics within 0.6 eV only by the alteration of alkyl chain length [14]. At the same time, introduction of fluoro-alkyl substituent leads to drastic decrease in the energy of their highest occupied molecular orbitals (HOMO) and lowest unoccupied molecular orbitals (LUMO) [14-15].

To facilitate the development of sensitizers owing to enormous structural possibilities, state-of-art theoretical calculations using Gaussian program package have gained the good deal of attentions in the recent past [16-17]. We have recently shown that amongst several hybrid functional available under density functional theory (DFT), there is a need for the judicious selection of optimum functional for predicting the energetics and electronic absorption spectrum of unsymmetrical squaraine dye [18]. To screen out the optimum molecular structure especially dyes having capability of photon harvesting in the far-red to NIR region, theoretical prediction of energy of dye molecules in the ground and excited states along with the electronic absorption spectra have been found to be extremely useful. Aim of the present investigation was to design and develop followed by selection of suitable molecular structure having minimum driving force for electron injection by the excited dye molecules to the conduction band (CB) of nanoporous TiO_2 which is highly required for the development of NIR sensitizers. For this purpose, we have selected some model far-red sensitizers belonging to the squaraine dye family having the molecular structure shown in the Fig.1. In parallel, these sensitizing molecules were synthesized and characterized also to correlate the theoretical results with the experimental values. Calculated results on energy of molecules in the ground and excited states, band gap, absorption maximum for these molecules were then compared with experimentally observed values to find the optimum molecular structure with smallest driving force for electron injection.

2. Experimental

2.1 Materials and methods

All the chemicals for synthesis or solvents are of analytical/spectroscopic grade and used as received without further purification. Synthesized squaraine (SQ)-dyes and dye intermediates were analysed by high performance liquid chromatography (HPLC) for purity, matrix assisted laser desorption and ionization (MALDI)-time-of-flight (TOF)-mass and fast ion bombardment (FAB)-mass spectrometry in the positive ion monitoring mode and nuclear magnetic resonance (NMR) spectroscopy (JEOL, 500 MHz) using Tetramethylsilane (TMS) as internal standard for structural elucidation. Electronic absorption spectroscopic investigations were conducted using UV–visible spectrophotometer (JASCO model V550). To construct the energy diagram for the dyes, HOMO energy level was estimated from the photoelectron spectroscopy in air (PESA, model AC3, Riken Keiki, Japan) while the LUMO energy level was estimated using the relation LUMO = HOMO + Eg, where, Eg is the optical band gap. Eg was estimated from the onset of the optical absorption. Theoretical quantum chemical calculations for the structural optimization as well as electronic absorption spectra for the far-red sensitizing squaraine dyes used in this work were conducted on Dell work-station using Gaussian G09 program package [19]. Calculation was done in both of the isolated molecule in gaseous state as well as in solution in the framework of the self-consistent reaction field polarizable continuum model (PCM) [20]. Ethanol was used as solvent not only for the electronic structure calculation but also experimental measurement of solution state electronic absorption spectra and preparation of dye-bath solution for the DSSC fabrication also.

DSSCs were fabricated using Ti-Nanoxide D paste (Solaronix SA) which was coated on a Low E glass (Nippon Sheet Glass Co., Ltd.) by a doctor blade. The substrate was then baked at 450◦C to fabricate TiO_2 layers of about 10 μm thickness. The substrate was dipped in the Ethanolic solution of the respective dyes in the presence of chenodeoxycholic acid (CDCA) for 4 hours. The dye concentration was fixed to be 0.25 mM while CDCA concentration was 25 mM. A Pt sputtered SnO_2/F layered glass substrate was employed as the counter electrode. Electrolyte containing LiI (500 mM), iodine (50 mM), t-butylpyridine (580 mM), MeEtIm-DCA (ethylmethylimidazolium dicyanoimide) (4:6, wt/wt) (600mM) in acetonitrile was used to fabricate the DSSC. A Himilan film (Mitsui-DuPont Polychemical Co., Ltd.) of 25 μm thickness was used as a spacer. The cell area was 0.25cm^2 which was precisely defined using a black metal mask.

The photovoltaic performances of the cells were measured using a solar simulator (CEP-2000 Bunko Keiki Co. Ltd, Japan) equipped with a xenon lamp (Bunko Keiki BSO-X150LC) used as a source of simulated solar irradiation at 100 mW/cm^2, AM 1.5 G. The power of the light exposure from the solar simulator was also adjusted with an amorphous Si photodetector (Bunko Keiki BS-520 S/N 353) to avoid the optical mismatch between the calibration diode and the DSSCs. The photocurrent action spectra was measured as a function of wavelength from 300 to 800 nm for the TCO-less BC-DSSCs with a constant photon flux of 1×10^{16} photon/cm^2 at each wavelength in DC mode using the action spectrum measurement system connected to the solar simulator (CEP-2000, Bunko Keiki, Japan). Cell area was maintained precisely using a black metal mask having area of 0.2025 cm^2 to measure the photovoltaic performance.

2.2 Synthesis of sensitizing dyes

Direct ring carboxy functionalized indole derivative 2,3,3-trimethyl-3H-indole-5-carboxylic acid used as common anchoring group for the all of the squaraine dyes used in this work was synthesized following the method reported by Pham et al. [21]. Details of the synthesis and characterization of this intermediate has published by us previously also [22]. Symmetrical squaraine dye **SQ-1** and **SQ-2** were synthesized as per our earlier publication [14]. Unsymmetrical squaraine dyes **SQ-6 and SQ-7** have been synthesized following the methodology adopted by Oswald et al. [23] and our earlier publication [24]. Symmetrical squaraine dyes bearing varying fluoroalkyl substituents (**SQ-3**, **SQ-4** and **SQ-5**) have been synthesized as per the synthetic scheme shown in the Fig. 2.

2.2.1 Synthesis of intermediate 5-Carboxy-2,3,3-trimethyl-1-pentafluorobutyl-3H-indolium iodide [2]

1.23 g (6 mmol) of 2,3,3-trimethyl-3H-indole-5-carboxylic acid and 1,1,1,2,2-pentafluoro-4-iodobutane (4.9 gm, 18 mmol) were dissolved in 50 ml of methoxy propionitrile and reaction mixture was heated at 140^{o}C for 18 hours under nitrogen. After completion of the reaction, solvent was evaporated and the crude product was washed with ample diethyl ether giving 1.3 g (2.7 mmol) of titled compound as brown powder in 45 % yield having 99 % purity as confirmed by HPLC. FAB-mass (measured m/z: 351.0; calculated m/z: 350.31) confirms the successful synthesis of this dye intermediate.

2.2.2 Synthesis of intermediate 5-Carboxy-2,3,3-trimethyl-1-Nonafluorohexyl-3H-indolium iodide [3]

1.23 g (6 mmol) of 2,3,3-trimethyl-3H-indole-5-carboxylic acid and 1,1,1,2,2,3,3,4,4-Nonafluoro-6-iodohexane (4.5 gm, 12 mmol) were dissolved in 50 ml of methoxy propionitrile and reaction mixture was heated at 140^{o}C for 48 hours under nitrogen. After

completion of the reaction, solvent was evaporated and the crude product was washed with ample diethyl ether giving 1.3 g (2.2 mmol) of titled compound as brown powder in 38 % yield having >98 % purity as confirmed by HPLC. FAB-mass (measured m/z: 451.0; calculated m/z: 450.31).

2.2.2 Synthesis of intermediate 5-Carboxy-2,3,3-trimethyl-1-Tridecafluorohexyl-3H-indolium iodide [4]

2,3,3-trimethyl-3H-indole-5-carboxylic acid (2.1 g, 10 mmol) and 1,1,1,2,2,3,3,4,4, 5,5,6,6-Tridecafluoro-8-iodooctane (7.1 gm, 15 mmol) were dissolved in 50 ml of methoxy propionitrile and reaction mixture was heated at 140^{o}C for 96 hours under nitrogen. After completion of the reaction, solvent was evaporated and the crude product was washed with ample diethyl ether giving 2.5 g (3.7 mmol) of titled compound as brown powder in 37 % yield having >99 % purity as confirmed by HPLC. FAB-mass (measured m/z: 551.0; calculated m/z: 550.1) confirms the identity of the synthesized intermediate compound.

2.2.3. Synthesis of symmetrical squaraine dye SQ-3

In a round bottom flask fitted with condenser 550 mg (1.7 mmol)) of 5-Carboxy-2,3,3-trimethyl-1-pentafluorobutyl-3H-indolium iodide (**2**) and squaric acid (50 mg, 0.5 mmol) were dissolved in 40 ml of dehydrated toluene-butanol (1:1 v/v) mixture. Reaction mixture was heated at reflux using Dean-Stark trap for 12 hours. After the completion of reaction, solvent was evaporated and crude product was purified by silica-gel flash column chromatography using chloroform-methanol as eluting solvent. 230 mg (0.3 mmol) of final titled compound was obtained as blue solid in 99% purity as confirmed by

HPLC and in 68% yield. FAB-mass (Calculated 776.19 and observed 776.0) and ^{1}H NMR (500 MHz, DMSO-d6): δ 1.57 (s, 6H), 2.77 (m, 2H), 4.46 (m, 2H), 5.91 (s, 1H), 7.42 (d, 1H), 7.98 (d, 1H), 8.03 (s, 1H) confirms the successful synthesis of the symmetrical squaraine dye **SQ-3**.

2.2.3. Synthesis of symmetrical squaraine dye SQ-4

In a round bottom flask fitted with condenser 420 mg (0.72 mmol) of 5-Carboxy-2,3,3-trimethyl-1-Nonafluorohexyl-3H-indolium iodide (**3**) and squaric acid (36 mg, 0.36 mmol) were dissolved in 40 ml of dehydrated toluene-butanol (1:1 v/v) mixture. Reaction mixture was heated at reflux using Dean-Stark trap for 18 hours. After the completion of reaction, solvent was evaporated and crude product was purified by silica-gel flash column chromatography using chloroform-methanol as eluting solvent. 190 mg (0.2 mmol) of titled compound was obtained as blue solid in > 98% purity as confirmed by HPLC and in 54 % yield. FAB-mass (Calculated 976.65 and observed 976.0) and ^{1}H NMR (500 MHz, DMSO-d6): δ 1.71 (s, 6H), 2.81 (t, 2H), 4.53 (m, 2H), 5.92 (s, 1H), 7.45 (d, 1H), 7.98 (d, 1H), 8.05 (s, 1H) confirms the successful synthesis of the symmetrical squaraine dye **SQ-4**.

2.2.3. Synthesis of symmetrical squaraine dye SQ-5

In a round bottom flask fitted with condenser 540 mg (0.8 mmol) of 5-Carboxy-2,3,3-trimethyl-1-Tridecafluorohexyl-3H-indolium iodide **(4)** and squaric acid (40 mg, 0.4 mmol) were dissolved in 40 ml of dehydrated toluene-butanol (1:1 v/v) mixture. Reaction mixture was heated at reflux using Dean-Stark trap for 18 hours. After the completion of

reaction, solvent was evaporated and crude product was purified by silica-gel flash column chromatography using chloroform-methanol as eluting solvent. 160 mg (0.14 mmol) of final titled compound was obtained as blue solid in 99% purity as confirmed by HPLC and in 34 % yield. FAB-mass (Calculated 1176.68 and observed 1177.0) and ^{1}H NMR (500 MHz, DMSO-d6): δ 1.69 (s, 6H), 2.78 (m, 2H), 4.53 (m, 2H), 5.91 (s, 1H), 7.45 (d, 1H), 7.98 (d, 1H), 8.04 (s, 1H) confirms the successful synthesis of the symmetrical squaraine dye **SQ-5**.

3. Results and discussion

3.1 Optical characterizations

Electronic absorption spectra of various squaraine dyes in ethanol solution have been shown in the Fig. 3. It can be seen that all of the squaraine dyes used in this work exhibit sharp and intense light absorption in the far-red (550 nm-700 nm) with very high molar extinction coefficient (ε = 2-3 X 10^5 $dm^3mol^{-1}cm^{-1}$) along with narrow (23-27 nm) full width at half maximum (FWHM). Appearance of this sharp absorption which is associated with the π-π^* electronic transition with small shoulder is a typical characteristics of the squaraine dyes. At the same time, this π-π^* electronic transitions for the unsymmetrical squaraine dyes (SQ-6 and SQ-7) have been found to exhibit about 10 nm of the blue-shifted absorption maximum (lmax) as compared to its symmetrical dye counterparts (SQ-1 and SQ-2). This could be explained considering the fact that unsymmetrical squaraine dyes lack one –COOH group and π-electron of which is in the direct conjugation with the indole ring of main π-framework leading to decreased effective π-conjugation of the dye. Interestingly, it has been found that even in the same

molecular framework in symmetrical squaraine dyes, there is a small blue shift (4 nm) in dyes bearing large electron withdrawing fluoroalkyl contents (SQ-3, SQ-4 and SQ-5). Although exact reason is not clear, but it could be attributed enhanced extent of inter-molecular hydrogen bonding leading to formation of H-aggregated species in the solution. Kim et al have also observed the formation of blue shifted H-aggregates formed by squaraine dyes on SnO_2 surface absorbing in the lower wavelength regions [25].

Squaraine dyes are also known to exhibit the strong fluorescence owing to their relatively small fluorescence life-time. At the same time, intersection and electronic absorption and fluorescence emission spectrum also known as $E_{o\text{-}o}$ transition has been used to estimate the optical band gap of the sensitizers. In fact, optical absorption edge has been used to estimate the calculation of optical band gap and this is true for materials having sharp absorption. In the cases when absorption spectrum is broader, sometimes it is difficult to clearly assign the absorption edge. In such a situation, assignment of Eg by $E_{o\text{-}o}$ transition seems to more reliable and accurate. Figure 4 shows the fluorescence emission spectrum for various squaraine dyes used for the present investigation. It can be seen from Fig 4 that emission spectra of the squaraine dyes are the mirror image of the absorption spectra shown in the Fig. 2 having nearly similar emission maxima between the 674-680 nm. The optical parameters based on measurement of absorption and emission spectrum is summarized in the table 1. The difference between the absorption and emission maximum also known as Stokes shift is relatively smaller (30-45 nm) as compared to most commonly used D-π-A sensitizers [26] and polymers [27] (> 100 nm).

This small stokes shift indicates the conformational rigidity of squaraine dye molecules in the solution.

3.2 Theoretical calculations

One of beauty of DSSC is freedom for designing organic sensitizers having immense structural possibility and various semi-empirical and ab-initio methods have been developed to achieve this goal and save the valuable time of the synthetic chemists. The ab-initio methods for electronic structure calculations have both pros and cons. It does not need any experimental parameters and is relatively more accurate but it needs the high computational cost as compared to semi-empirical methods. Amongst electronic structure calculation methodologies, density functional theory (DFT) has emerged as one of the reliable methods for the theoretical treatment of suitability of dye molecular structure as a photosensitizer. DFT considers the electron and lone pair correlations like ab-initio methods but only at the computation cost of HF. Its time dependent extension (TD-DFT) has been demonstrated to provide reliable values for the excitation energies with the standard correlation functional which has been extensively used for the design and development of new dyes for the DSSCs [28-29]. Apart from the high molar extinction coefficient, energetic match with respect to oxide semiconductor and redox electrolyte, distribution of electron density in LUMO and its sufficient diversion at the anchoring group are highly desired properties of a suitable sensitizer of DSSCs.

First of all, one of the proposed model far-red sensitizing dye (SQ-6) was subjected to ground state electronic structure calculation pertaining to the structural optimization in gaseous state. In order to make a judicious balance between the

computation cost and accuracy, structural optimization was conducted using diffuse basis set (6-311G) and applying the DFT and varying the different functionals employed in the Gaussian program package. Results of the calculation in terms the optimized minimum energy structure along with the electronic distribution in its HOMO and LUMO are shown in the Fig. 5. It can be clearly seen from Fig. 5 that electron density in HOMO is mainly centralized at central squaraine core which is associated with the π-framework of the dye. On the other hand, electron density distribution in LUMO associated with π* MO is also delocalized over the entire molecular framework having sufficient diversion of electron density at the –COOH anchoring group present in the indole ring. Such diversion indicates the sufficient electronic coupling of this dye with the oxide semiconductor leading to the facile electron injection upon the photoexcitation.

After optimization of geometry sensitizer SQ-6 was also subjected to the excited state electronic structure calculation using TD-DFT and different functionals at 6-311G level This calculation was performed both for the isolated molecule in gaseous state as well as in ethanol solution using solvent polarization continuum model (PCM) in order to simulate the electronic absorption spectra [20]. Excited state TD-DFT calculations provide information about the electronic transitions, molar extinction coefficients (ε) and oscillator strength (f) and dipole moment (Debye, D) of the molecule under investigation. Calculated electronic absorption spectra of SQ-6 using different functionals, ethanol solvent and its experimental result are shown in the Fig.5 along with calculated parameters as shown in the table 2.

A perusal of Fig. 6 indicates SQ-6 exhibits intense electronic transition in the far-red region having oscillator strength associated with main π-π* electronic transition from the HOMO-LUMO. From table 2, it is clear that under TD-DFT, most commonly employed hybrid functionals B3LYP and B3PW91 in isolated gaseous state gives nearly similar results in terms of the energy of HOMO and LUMO along with the λ_{max}. Interesting, in the case of same utilization of same functional and theory, implementation of solvent assisted PCM model not only leads to decrease in HOMO from – 5.08 eV to – 5.24 eV but also red shift in the λ_{max} from 557 nm to 579 nm. This indicates that implementation of solvents brings the calculated results more near to the experimentally observed values. In the theoretical investigations pertaining to Ru and Os based sensitizers, Gullemoles et al [30] have advocated that inclusion of solvents effects is necessary and gives relatively better results. Although BPV86 functionals gives relatively better result for the λ_{max} but calculated energetics are far from the experimentally observed values. At the same time, LSDA seems to be a good functional in terms of the prediction of HOMO energy level and λ_{max} even without the implementation of solvent model. Theoretical calculation using LSDA gives only a difference of 0.15 eV for HOMO energy and 39 nm for λ_{max} as compared to the experimentally measured values of the dye SQ-6 indicating potentiality of such methodology towards the theoretical prediction of absorption spectra and energetics for the design and development of novel NIR sensitizers.

3.3 Energy band diagram

Sensitizing dyes are considered to be the heart of DSSCs since they are actual photon harvester play their pivotal role in controlling the overall power conversion efficiency. Design of a novel sensitizer for DSSC applications is based on the judicious control of energy level of HOMO and LUMO of dyes with respect to the energy level of the redox couple (I^-/I_3^-) and conduction band (CB) of TiO_2, respectively. Especially for the NIR photosensitization, there is a need of minimization of the energy gap for electron injection to the CB of the TiO_2 and dye regeneration from the redox electrolyte to the oxidized dye. Therefore, increasing the wavelength of the dyes needs relatively more careful and strict control of the energetics due to their decreased Eg. The energy band diagram of the various squaraine based sensitizers along with the energy level of the TiO_2 and I^-/I_3^- redox couple has been shown in the Fig. 6. Redox potential of I_3^-/I^- redox couple has been reported to be 0.44 V vs. NHE or - 4.9 eV with respect to the vacuum level. [31]. At the same time, CB of TiO_2 was taken to be - 4.0 eV considering the most negative quasi Fermi level corresponding to the flat band potential of TiO_2 (0.7 V vs. SCE) [32].

To construct this energy diagram the HOMO energy level of the squaraine dyes were estimated from photoelectron yield spectroscopy while LUMO energy level was estimated by adding energy corresponding to the Eg of the dye to the HOMO energy level. Eg was estimated from the intersection of electronic absorption and fluorescence emission spectra of respective dyes as shown in the table 1. A perusal of Fig. 7 clearly corroborates that squaraine dyes exhibit energetic cascade with respect to the CB of TiO_2

and energy level of redox electrolyte ensuring electron injection and dye regeneration. It can be seen that by judicious molecular design in terms of molecular asymmetry and extent of electron withdrawing $(-CF_2)_n$ moieties in the substituents it is possible to fine tune the energetics at about 0.1 eV energy level. At the same time we are able to design a novel dye having minimum thermodynamic energy barrier for electron injection to bring as lower as 0.16 eV. Interestingly, theoretically calculated values of HOMO energy level (shown in parentheses) exhibit very good agreement with the experimentally determined values of respectively dyes having only a difference of 0.02 eV to 0.15 eV.

3.4 Photovoltaic Characterizations

Current–voltage (I–V) characteristics of DSSCs based on the different squaraine dyes used in this work under standard global AM 1.5 simulated solar irradiation have been shown in Fig. 8 along with their photovoltaic parameters deduced from the I-V characteristics as shown in the table 3. A perusal of Fig. 8 and table 3 clearly indicates that all of the designed squaraine sensitizers are capable of harvesting photons and exhibit the photovoltaic behavior. Unsymmetrical squaraine dyes (SQ-6 and SQ-7) having exactly similar molecular framework and alkyl chain length exhibit superior photovoltaic performance as compared to their corresponding symmetrical dye counterparts (SQ-1 and SQ-2). This could be attributed to the unidirectional flow of electron after the photoexcited electron injection to the nanoporous TiO_2. Such unidirectional flow assisted enhanced photovoltaic performance in unsymmetrical squaraine dyes has been advocated and reported by Alex et al and many researchers also [10, 22, 33].

It is interesting to note SQ-6 and SQ-7 are very much similar in the molecular structure differing only in the relative positioning of side chain substituents. In spite of such a small difference in the molecular structure, the energy of their HOMO and LUMO is being altered by 0.1 eV and SQ-7 exhibits relatively improved photovoltaic performance as compared to SQ-6 giving external power conversion efficiency (η) of 4.01 % under simulated solar irradiation. It is worth to mention here that newly designed sensitizer SQ-5 with very small thermodynamic energy barrier for electron injection (0.16 eV) is able to exhibit the photovoltaic behavior. Upon simulated solar irradiation at AM 1.5 condition, SQ-5 exhibits a short circuit current density (Jsc) of 5.10 mA/cm2, open circuit voltage (Voc) of 0.57 V and fill factor (ff) of 0.69 leading to photoconversion efficiency of 2.02 %.

.

In order to elucidate the observed different Jsc for squaraine dyes under investigation along with having further insight about their photon harvesting behaviour, photo-current action spectra after the DSSCs fabrication was also measured and is shown in the Fig. 9. Photocurrent action spectrum is basically variation of incident photon to current conversion efficiency (IPCE) as a function of wavelength after the monochromatic light illumination. A symbatic photo-current action spectrum with electronic absorption spectrum confirms that the observed photocurrent in the device arises from the photo-excited electron injection. A perusal of the action spectra shown in Fig. 9 and electron absorption spectra (Fig. 3) clearly corroborates that the action spectrum is perfectly symbatic (nearly similar shape and peak maximum) with spectral broadening due to aggregate formation in solid state. The maximum of IPCE for

unsymmetrical squaraine dyes (SQ-6 & SQ-7) are pronounced (55 % & 57 %) as compared to their corresponding symmetrical squaraine dye counter parts (SQ-1 & SQ-2) with IPCE maxima at 53 % and 45 %, respectively and are in accordance with observed Jsc in I-V characteristics. The observation of photon harvesting for DSSCs using SQ-5 exhibiting IPCE of 36 % at the peak indicates that SQ-5 is still able inject electron in the CB of TiO_2 after photoexcitation even with such a small energy barrier 0.16 eV. This information seems to be quite useful in order to design and develop novel squaraine sensitizers having photon harvesting in NIR region and attain panchromatic photon harvesting in combination with the potential visible light sensitizing dyes.

Conclusions

A combined theoretical and experimental approach has been implemented to design and develop NIR dyes towards their application as photosensitizers for the DSSCs. With the help of logical molecular design, we are able to fine tune the energetics of the HOMO and LUMO energy level of far-red sensitizing dyes by 0.1 eV level. It has been found that implementation of PCM model in calculation at TD-DFT/B3PW91 platforms for theoretical calculations leads to the 23 nm bathochromic shifts in the λ_{max} and 0.15 eV downward shift in HOMO energy level as compared to calculation in gaseous state leading to better match between experimentally observed and theoretically calculated values. Interestingly calculation performed at TD-DFT/LSDA level gives calculated results which are most nearest to the experimental values even without implementing the solvent model seems to be a good balance between the computational cost and accuracy. Symmetrical squaraine dye SQ-5 exhibits the IPCE of 36 % at the peak even with energy

barrier for electron injection of 0.16 eV indicates the possibility of further molecular design of novel sensitizers having the capability of photon harvesting in the NIR wavelength region.

Acknowledgement

This work was partially supported by JSPS grant-in-aid for scientific research-C (Grant number-26410206) and being gratefully acknowledged.

References

[1] M. Grätzel, Solar energy conversion by dye-sensitized photovoltaic cells, Inorganic Chemistry 44 (2005) 6841-6851.

[2] S. Ito, T.N. Murakami, P. Comte, P. Liska, C. Grätzel, M.K. Nazeeruddin, M. Grätzel, Fabrication of thin film dye sensitized solar cells with solar to electric power conversion efficiency over 10%, Thin Solid Films 516 (2008) 4613-4619.

[3] A. Mishra, M.K.R. Fischer, P. Bäuerle, Metal-Free organic dyes for dye-sensitized solar cells: from structure: property relationships to design rules, Angew. Chem. Int. Ed. 48 (2009) 2474-2499.

[4] M. Wang, C. Grätzel, S.M. Zakeeruddin, M. Grätzel, Recent developments in redox electrolytes for dye-sensitized solar cells, Energy and Environmental Science 5 (2012) 9394-9405.

[5] S. Yun, A. Hagfeldt, M. Tingli, Pt-free counter electrode for dye-sensitized solar cells with high efficiency, Advanced Materials. 24 (2014) 6210-6237.

[6] F. Gao, Y. Wang, D. Shi, J. Zhang, M. Wang, X. Jing, R. H. Baker, P. Wang, S.M. Zakheeruddin, M. Grätzel, Enhance the optical absorptivity of nanocrystalline TiO_2 film with high molar extinction coefficient ruthenium sensitizer for high performance dye-sensitized solar cell, Journal of American Chemical Society 130(32) (2008) 10720-10728.

[7] A. Yella, H.W. Lee, HN. Tsao, C. Yi, A.K. Chandiran, M.K. Nazeeruddin, E.W.G. Dian, C.Y. Yeh, S.M. Zakeeruddin, M. Grätzel, Porphyrin-sensitized solar cells with cobalt (Ⅱ/Ⅲ) based redox electrolyte exceed 12 percent efficiency, Science 334 (2011) 629-634.

[8] S. Mathew, A. Yella, P. Gao, R.H. Baker, B.F.E. Curchod, N.A. Astani, I. Tavernelli, U. Rothlisberger, Md. K. Nazeeruddin, M. Grätzel, Dye-sensitized solar cells with 13% efficiency achieved through the molecular engineering of porphyrin sensitizers, Nature Chemistry 6 (2014) 242-247.

[9] K. Kakiage, Y. Aoyama, T. Yano, T. Otsuka, T. Kyomen, M. Unno, M. Hanaya, An achievement of over 12 percent efficiency in an organic dye-sensitized solar cell, Chem. Commun. 50 (2014) 6379-6381.

[10] J.H. Yum, P. Walter, S. Huber, D. Rentsch, T. Geiger, F. Nuësch, F.D. Angelis, M. Grätzel, M.K. Nazeeruddin, Efficient far red sensitization of nanocrystalline TiO2 films by an unsymmetrical squaraine dye, J. Am. Chem. Soc. 129 (2007) 10320-10321.

[11] G.M. Shivashimpi, S.S. Pandey, R. Watanabe, N. Fujikawa, Y. Ogomi, Y. Yamaguchi, S. Hayase, Novel unsymmetrical squaraine dye bearing cyanoacrylic acid anchoring group and its photosensitization behavior, Tetrahedron Letter 53 (2012) 5437-5440.

[12] S.S. Pandey, R. Watanabe, N. Fujikawa, G.M. Shivashimpi, Y. Ogomi, Y. Yamaguchi, S. Hayase, Effect of extended π-conjugation on photovoltaic performance of dye sensitized solar cells based on unsymmetrical squaraine dyes, Tetrahedron 69 (2013) 2633-2639.

[13] Z. Yan, S. Guang, X. Su, H. Xu, Near-infrared absorbing squaraine dye for solar cells: Relationship between architecture and performance, J. Physical. Chemistry. 113 (2012) 8894-8900.

[14] S.S. Pandey, T. Inoue, N. Fujikawa, Y. Yamaguchi, S. Hayase, Substituent effect in direct ring functionalized squaraine dyes on near infra-red sensitization of nanocrystalline TiO_2 for molecular photovoltaics, Journal of Photochemistry and Photobiology A: Chemistry 214 (2010) 269-275.

[15] S.S. Pandey, T. Inoue, N. Fujikawa, Y. Yamaguchi, S. Hayase, Alkyl and fluoro-alkyl substituted squaraine dyes: A prospective approach towards development of novel NIR sensitizers, Thin Solid Films 519 (2010) 1066-1071.

[16] M.K. Nazeeruddin, F.D. Angelis, S. Fantacci, A. Selloni, G. Viscardi, P. Liska, S. Ito, B. Takeru, M. Grätzel, Engineering of efficient panchromatic sensitizers for nanocrystalline TiO_2-based solar cells, J. Am. Chem. Soc. 123 (2001) 1613-1624.

[17] J.E. Monat, J.H. Rodriduez, J.K. McCusker, Ground- and excited-state electronic structures of the solar cell sensitizer bis(4,4‘-dicarboxylato-2,2‘-bipyridine) bis(isothiocyanato) ruthenium(Ⅱ) J. Phys. Chem. A 106 (2002) 7399-7406.

[18] Y. Yamaguchi, S.S. Pandey. N. Fujikawa, Y. Ogomi, S. Hayase, A combined theoretical and experimental approaches towards designing NIR dyes for dye-sensitized solar cells, Journal of Engineering Science and Technology. (2014) 51-65.

[19] M.J. Frisch, G.W. Trucks, H.B. Schlegel, G.E. Scuseria, M.A. Robb, J.R. Cheeseman, G. Scalmani, V. Barone, B. Mennucci, G.A. Petersson, H. Nakatsuji, M. Caricato, X. Li, H.P. Hratchian, A.F. Izmaylov, J. Bloino, G. Zheng, J.L. Sonnenberg, M. Hada, M. Ehara, K. Toyota, R. Fukuda, J. Hasegawa, M. Ishida, T. Nakajima, Y. Honda, O. Kitao, H. Nakai, T. Vreven, J.A. Montgomery Jr., J.E. Peralta, F. Ogliaro, M. Bearpark, J.J. Heyd, E. Brothers, K.N. Kudin, V.N. Staroverov, R. Kobayashi, J. Normand, K. Raghavachari, A. Rendell, J.C. Burant, S. S. Iyengar, J. Tomasi, M. Cossi, N. Rega, J.M. Millam, M. Klene, J.E. Knox, J.B. Cross, V. Bakken, C. Adamo, J. Jaramillo, R Gomperts, R.E. Stratmann, O. Yazyev, A.J. Austin, R. Cammi, C. Pomelli, J.W. Ochterski, R.L. Martin, K. Morokuma, V. G. Zakrzewski, G.A. Voth, P. Salvador, J.J. Dannenberg, S. Dapprich, A.D. Daniels,

O. Farkas, J. B. Foresman, J.V. Ortiz, J. Cioslowski, D.J. Fox, Gaussian 09, Revision A.02; Gaussian Inc.: Wallingford CT, 2009.

[20] J. Tomasi, B. Mennucci, R. Cammy, Quantum mechanical continuum solvation models, Chemical Reviews. 105 (2005) 2999-3093.

[21] W. Pham, W.F. Lai, R. Weissleder, C.H. Tung, High efficiency synthesis of a bioconjugatable near-infrared fluorochrome, Bioconjugate Chem. 14 (2003) 1048-1051.

[22] T. Inoue, S.S. Pandey, N. Fujikawa, Y. Yamaguchi, S. Hayase, Synthesis and characterization of squaric acid based NIR dyes for their application towards dye-sensitized solar cells, Journal of Photochemistry and Photobiology A: Chemistry 213 (2010) 23-29.

[23] B. Oswald, L. Patsenker, J. Duschl, H. Szmacinski, O.S. Wolfbeis, E. Terpetschnig, Synthesis, spectral properties, and detection limits of reactive squaraine dyes, a new class of diode laser compatible fluorescent protein labels, Bioconjugate Chem. 10 (1991) 925-931.

[24] T. Morimoto, N. Fujikawa, Y. Ogomi, S.S. Pandey, T. Ma, S. Hayase, Design of far-red sensitizing squaraine dyes aiming towards the fine tuning of dye molecular structure, Journal of Nanoscience and Nanotechnology. (2015) (In press).

[25] C. Kim, H. Choi, S. Kim, C. Baik, K. Song, M.S. Kang, S.O. Kang, J. Ko, Molecular Engineering of organic sensitizers containing p-phenylenevinylene unit for dye-sensitized solar cells, J. Org. Chem. 73 (2008) 7072-7079.

[26] D.P. Hagberg, T. Marinado, K.M. Karlsson, K. Nonomura, P. Qin, G. Boschloo, T. Brinck, A. Hagfeldt, L. Sun, Tuning the HOMO and LUMO energy levels of organic chromophores for dye sensitized solar cells, J. Org. Chem. 72 (2007) 9550-9556.

[27] T. Dutta, K.B. Woody, S.R. Parkin, M.D. Watson, J. Gierschner, Conjugated polymers with large effective strokes shift: Benzobisdioxole-based poly (phenylene ethynylenes, J. Am. Chem. Soc. 131 (2009) 17321-17327.

[28] N. Santhanamoorthi, C.M. Lo, J.C. Jiang, Molecular design of porphyrins for dye-sensitized solar cells: A DFT/TDDFT study, J. Phys. Chem. Lett. 4 (2013) 524-530.

[29] M.K. Nazeeruddin, F.D. Angelis, S. Fantacci, A. Selloni, G. Viscardi, P. Liska, S. Ito, B. Takeru, M. Grätzel, J. Am. Chem. Soc. 127(48) (2005) 16835-16847.

[30] J.F. Gullemoles, V. Barone, L. Joubert, C.A. Adamo, Theoretical investigations of the ground and excited states of selected Ru and Os polypyridyl molecular dyes, Journal of Physical Chemistry A. 106 (2002) 11354-11360.

[31] Y. Ogomi, T. Kato, S. Hayase, Dye sensitized solar cells consisting of ionic liquid and solidification, J Photopolym. Sci. Technol. 19 (2006) 403-408.

[32] A. Hagfeldt, M Grätzel, Light-induced redox reactions in nanocrystalline systems, Chem. Rev. 95 (1995) 49-68.

[33] S. Alex, U. Santhosh, S. Das, Dye sensitization of nanocrystalline TiO2: enhanced efficiency of unsymmetrical squaraine dyes, J. Photochem. Photobiol. A 172 (2005) 63-71.

Figure captions

Figure 1. Structure of far-red sensitive squaraine dyes used in the present work.

Figure 2. Synthetic scheme for symmetrical squaraine dyes.

Figure 3. Electronic absorption spectra of squaraine dyes in ethanol solution (5 μM).

Figure 4. Fluorescence emission spectra of squaraine dyes in ethanol solution (5 μM).

Figure 5. Calculated stereograph (optimized structure), HOMO and LUMO orbital diagrams for SQ-6 using B3PW91 functional under DFT and 6-311G basis set.

Figure 6. Calculated electronic absorption spectra of SQ-6 in isolated gaseous state, using different functionals, solvent model using ethanol.

Figure 7. Energy band diagram for squaraine dyes along with the TiO_2 and iodine based redox electrolyte. Values shown in the parenthesis are the calculated values using LSDA functional under TD-DFT and 6-311G basis set.

Figure 8. Photovoltaic characteristics of DSSCs fabricated using different squaraine dyes under 100 mW/cm^2 simulated solar irradiation.

Figure 9. Photocurrent action spectra of the DSSCs based on different squaraine dyes after monochromatic light illumination.

Table 1. Optical properties for squaraine dyes in the ethanol solution.

Sensitizer	λ_{max} (Excitation) [nm]	λ_{max} (Emission) [nm]	E_{o-o} [nm]	Eg [eV]	Stokes shift [nm]	FWHM [nm]
SQ-1	645	674	659	1.88	29	24
SQ-2	642	674	659	1.88	32	25
SQ-3	638	674	658	1.88	36	24
SQ-4	638	674	658	1.88	36	24
SQ-5	638	678	658	1.88	40	24
SQ-6	635	680	656	1.89	45	27
SQ-7	636	678	656	1.89	42	23

Table 2. Calculated results for SQ-6 after the structural optimization with 6-311G basis set under DFT along with the experimental results.

Calculation parameters	**HOMO (eV)**	**LUMO (eV)**	**λ_{max} (nm)**	**Dipole moment (Debye)**	**Oscillator Strength (f)**
B3LYP	- 5.08	- 2.91	561	7.0537 D	1.4616
CAM-B3LYP	- 6.08	- 2.05	549	7.1960 D	1.5112
B3PW91	- 5.08	- 2.90	557	4.8922 D	1.4741
B3PW91-Ethanol	- 5.24	-3.02	579	2.6946 D	1.8950
LSDA	- 5.24	-3.87	597	4.8140 D	1.3110
BPV86	- 4.90	- 3.30	599	4.7156 D	1.2855
Experimental-Ethanol	- 5.39	- 3.50	636	-	-

Table 3. Photovoltaic parameters for the DSSCs fabricated using squaraine dyes under identical experimental conditition.

Squaraine sensitizers	Jsc (mA/cm^2)	Voc (V)	FF	η (%)
SQ-1	8.51	0.57	0.69	3.36
SQ-2	6.83	0.57	0.72	2.84
SQ-3	6.29	0.56	0.67	2.35
SQ-4	4.96	0.55	0.71	1.92
SQ-5	5.10	0.57	0.69	2.02
SQ-6	9.00	0.62	0.65	3.64
SQ-7	9.60	0.63	0.67	4.01

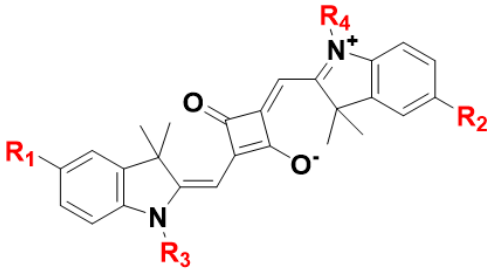

	R_1	R_2	R_3	R_4
SQ-1	CO_2H	CO_2H	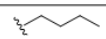	
SQ-2	CO_2H	CO_2H	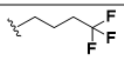	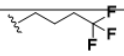
SQ-3	CO_2H	CO_2H	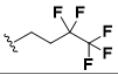	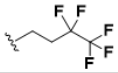
SQ-4	CO_2H	CO_2H	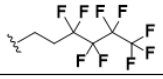	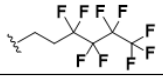
SQ-5	CO_2H	CO_2H		
SQ-6	CO_2H	H	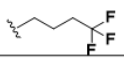	
SQ-7	CO_2H	H	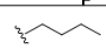	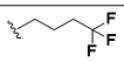

Figure. 1

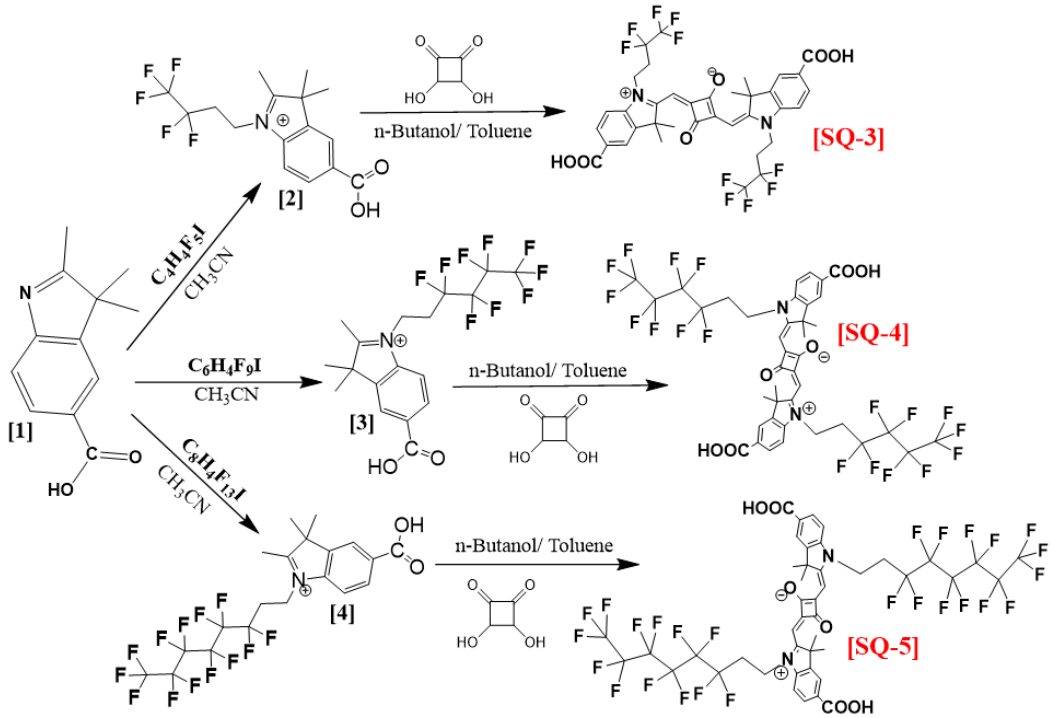

Figure. 2

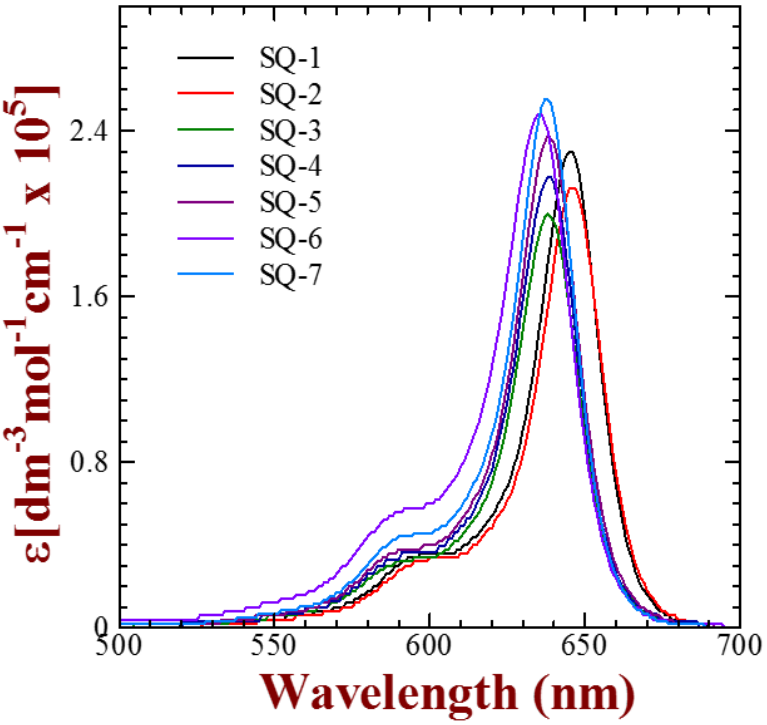

Figure. 3

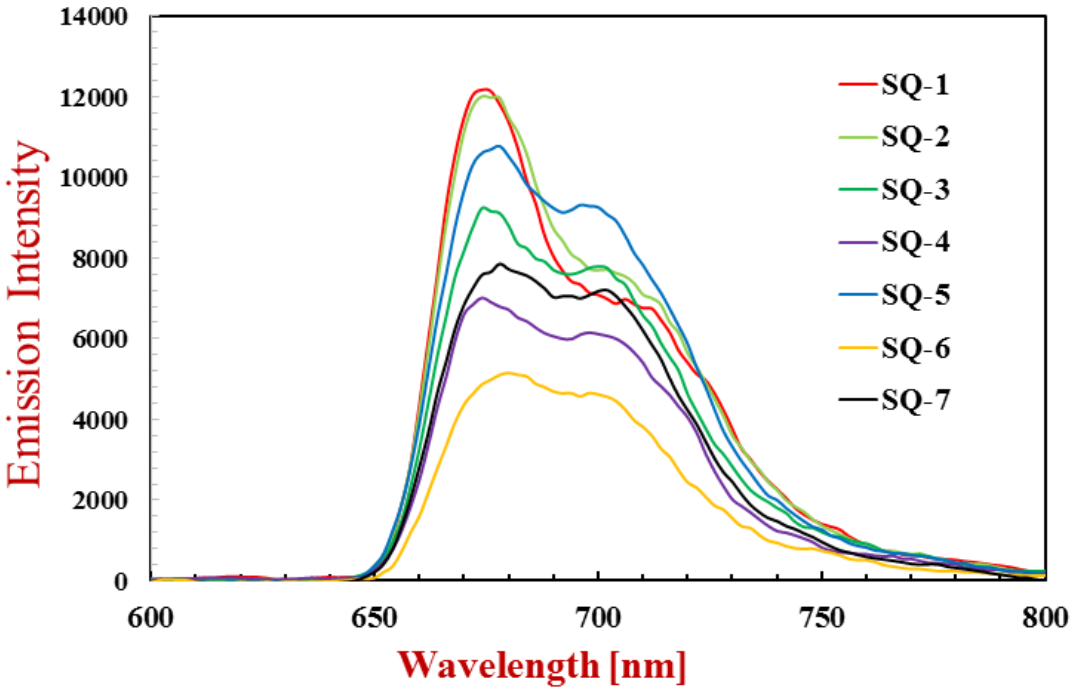

Figure. 4

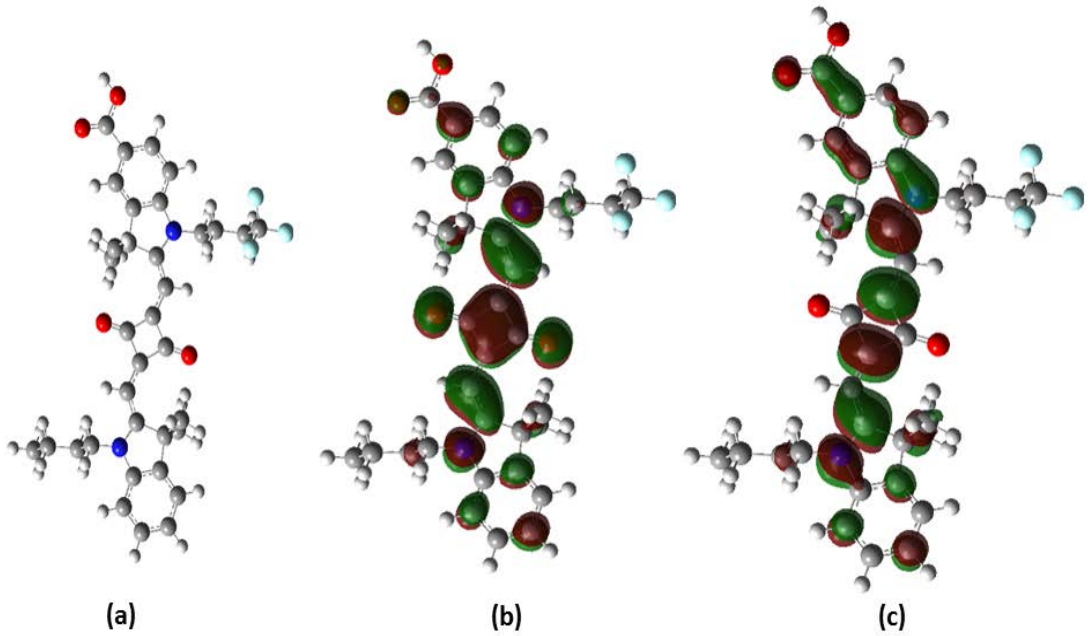

Figure. 5

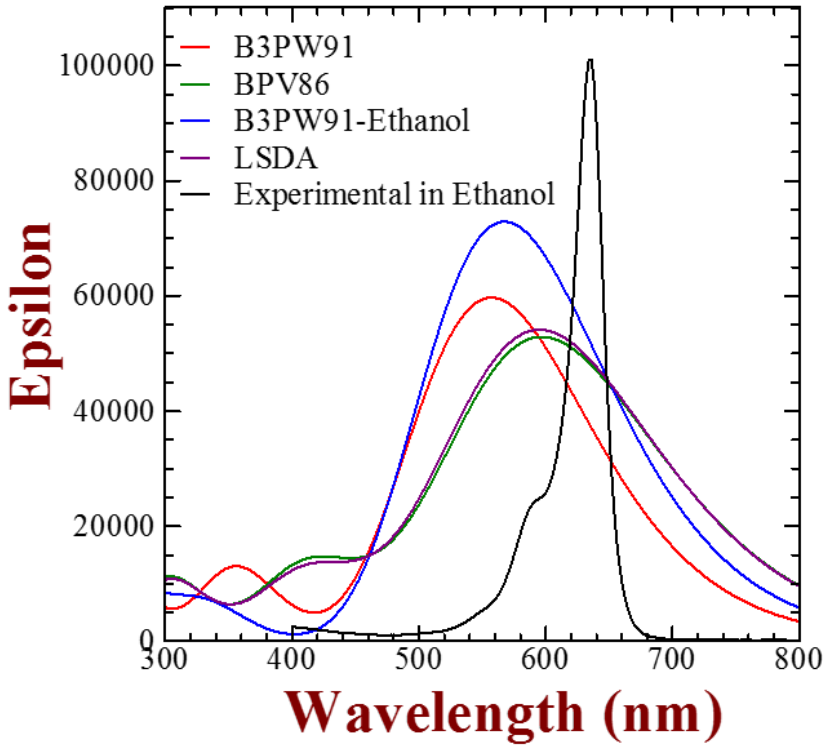

Figure. 6

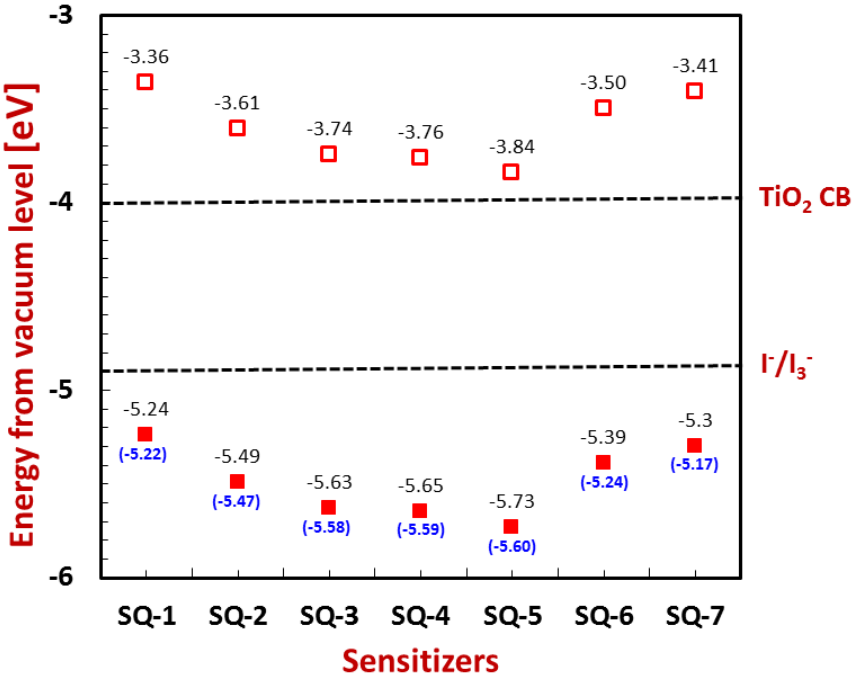

Figure. 7

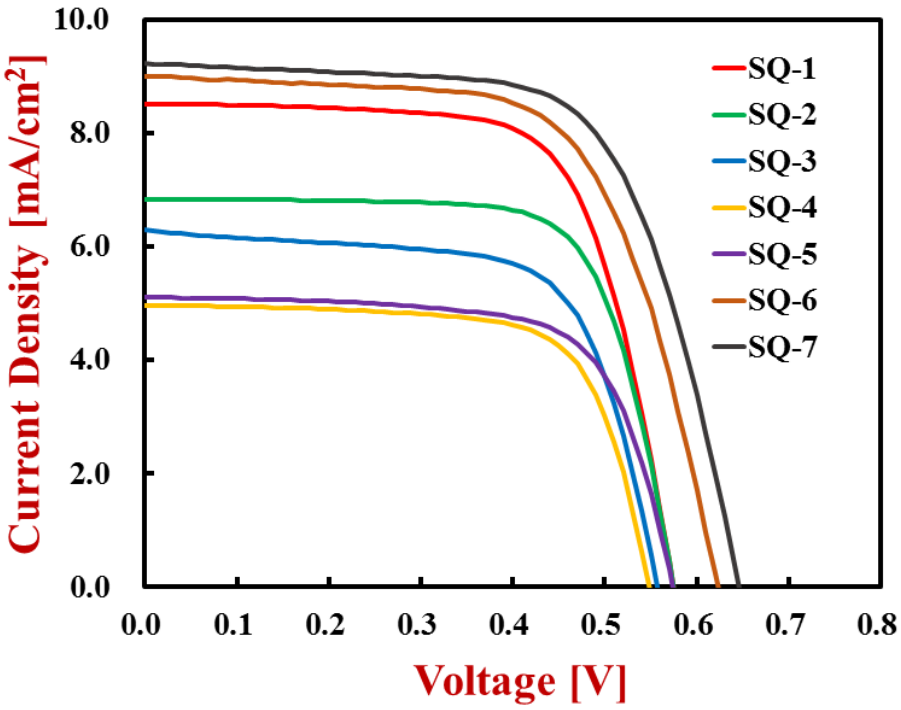

Figure. 8

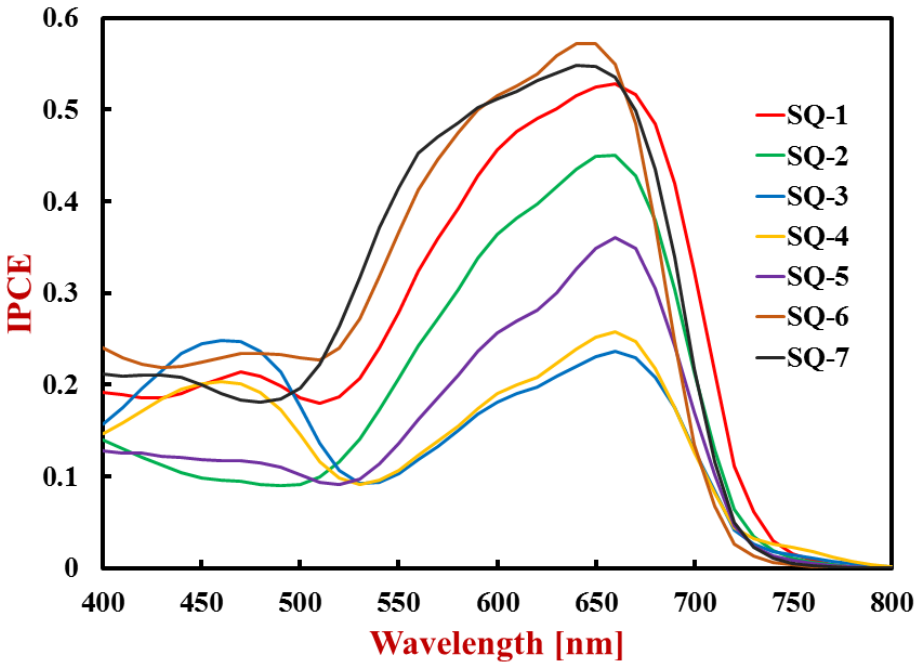

Figure. 9